Importance of O(^{3}P) Atoms and OH Radicals in Hydrocarbon Oxidation During the Nonthermal Plasma Treatment of Diesel Exhaust Inferred Using Relative-Rate Methods

JOHN HOARD,[1] TIMOTHY J. WALLINGTON,[1] RICHARD L. BRETZ,[1]
ALEXANDER MALKIN,[1] RAJESH DORAI,[2] MARK J. KUSHNER[3]

[1]*Ford Research Laboratory*, SRL-3083, P.O. Box 2053, *Dearborn*, *Michigan* 48121
[2]*Department of Chemical Engineering*, *University of Illinois at Urbana–Champaign*, 1406, W. *Green St.*, *Urbana*, *Illinois* 61801
[3]*Department of Electrical and Computer Engineering*, *University of Illinois at Urbana–Champaign*, 1406, W. *Green St.*, *Urbana*, *Illinois* 61801

Received 25 March 2002; accepted 12 February 2003

DOI 10.1002/kin.10122

ABSTRACT: The consumption of acetylene and propene during passage of simulated diesel exhaust through a nonthermal plasma at 453 K and atmospheric pressure was studied using experimental and computational techniques. Experimental observations of the relative decay rates of acetylene and propene and computer modeling of the chemical and physical processes in the plasma suggest that O(^{3}P) atoms and, to a lesser extent, OH radicals are the dominant species responsible for initiating hydrocarbon oxidation in this system. Results are discussed in terms of the gas-phase chemistry occurring during the nonthermal plasma treatment of diesel exhaust. © 2003 Wiley Periodicals, Inc. Int J Chem Kinet 35: 231–238, 2003

This work was performed as part of "CRADA PNL-089: New Technologies for Exhaust Emission Reduction" a cooperative project of the USCAR Low Emissions R&D Partnership, Pacific Northwest National Lab, and the U.S. Department of Energy.

Correspondence to: Timothy J. Wallington; e-mail: twalling@ford.com.

Present address of Rajesh Dorai: Varian Semiconductor Equipment Associates, 35 Dory Road, Gloucester, MA 01930.

Contract grant sponsor: Ford Motor Company.
Contract grant sponsor: National Science Foundation.
Contract grant number: CTS99-74962.

INTRODUCTION

Concerns about global climate change have increased the pressure on automobile manufacturers to increase vehicle fuel efficiency. While diesel engines offer improved fuel economy compared to gasoline vehicles, NO_x emissions from diesel engines may be difficult to control as per proposed future emissions standards. Modern spark-ignition engines operate at stoichiometry and NO_x emissions are controlled by a three-way catalytic converter. Diesel engines operate lean, and the exhaust contains substantial amounts of O_2 (typically 6–10%). The reduction of NO_x by a three-way catalyst in such oxidizing environments is difficult.

Nonthermal plasma discharge combined with a downstream catalyst is a technology under evaluation for use in the removal of NO_x from diesel exhaust [1–4]. Paradoxically, it is believed that the main function of the plasma in such systems is to *oxidize* NO to species such as NO_2 that are more easily *reduced* by the downstream catalyst [5]. The plasma also plays an important role in partially oxidizing hydrocarbons to species that act as efficient reductants on the catalyst [6–8].

The details of the gas-phase chemistry occurring in the plasma discharge of exhaust gas are not fully understood. It is well established that passage of O_2 through a nonthermal plasma leads to the formation of $O(^3P)$ atoms [9], which can react with organic compounds [10]. The $O(^3P)$ atom initiated oxidation of hydrocarbons in the presence of NO_x leads, directly and indirectly, to the generation of hydroxyl (OH) radicals. Hydroxyl radicals also initiate the oxidation of hydrocarbons leading to further OH radical formation via a chain mechanism [11]. While it is anticipated that $O(^3P)$ atoms and OH radicals are responsible for the majority of the oxidation of the organic compounds, this has yet to be demonstrated experimentally and the relative importance of $O(^3P)$ atoms and OH radicals is unclear. Diesel exhaust contains N_2, O_2 (6–10%), NO_x (100–1000 ppm, primarily as NO), H_2O (5–12%), CO_2 (5–13%), and hydrocarbons (100–1000 ppm). Electron impact can generate a variety of other reactive atomic (e.g., $O(^1D)$, $N(^4S)$, $N(^2D)$, and $N(^2P)$) and electronically excited molecular species (e.g., N_2 ($A^3\Sigma_u^+$) and O_2 ($^1\Delta_g$)). The role, if any, played by these species in hydrocarbon oxidation is unclear.

The goal of the present work was to provide insight into which species initiate the oxidation of hydrocarbons during plasma treatment of diesel exhaust. Experimental and computational techniques were employed. Results indicate that $O(^3P)$ atoms and, to a lesser extent, OH radicals are the dominant species responsible for initiating the oxidation of organic compounds in such systems.

EXPERIMENTAL AND COMPUTATIONAL DETAILS

Description of the Experiment

The work was performed using a flow bench which blends gases to simulate diesel-engine exhaust [12]. Figure 1 is a schematic of the experimental system. NO, O_2, C_3H_6, and C_2H_2 were mixed in N_2 carrier. Liquid water was injected into the gas in heated lines. The plasma device was mounted in an oven maintained at 180°C. The effluent exiting the plasma/catalyst system was mixed with extra N_2 to prevent condensation of water and passed through measurement instrumentation at room temperature. Acetylene and propene concentrations were monitored using Mattson Nova Cygni 120 FTIR spectrometer operated at a spectral resolution of 0.25 cm^{-1} and equipped with a long path length (20.7 m) sampling cell [13]. Additional analytical instrumentation included Horiba Model FMA 220 oxygen analyzer, Horiba Model CLA-220 chemiluminescent NO_x analyzer (CLA), and Horiba Model FMA 220 Flame Ionization Detector for hydrocarbons (HC).

Table I lists the nominal composition of the gas blend used. This mixture approximates the gas composition of diesel-engine exhaust, although the HC concentration is about four times higher than that in

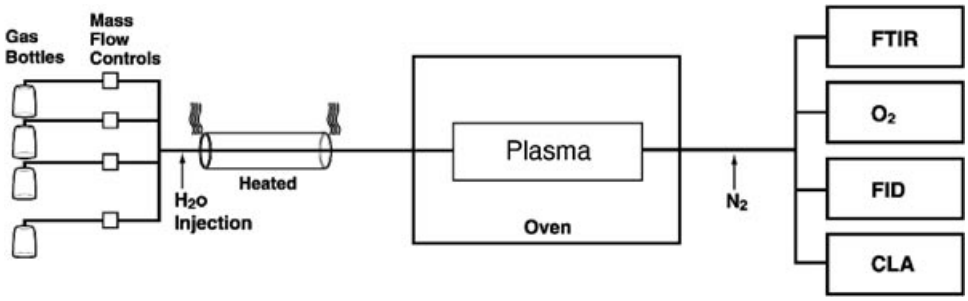

Figure 1 Schematic of test lab configuration (FTIR, Fourier transform infrared spectrometer; FID, flame ionization detector for hydrocarbons; CLA, chemiluminescence NO_x analyzer).

Table I Nominal Gas Composition Used in Present Work

Gas	Concentration
NO	260 ppm
O_2	8%
H_2O	2%
C_3H_6	1000 ppmC_1
C_2H_2	1000 ppmC_1
N_2	Balance

typical modern diesel-engine exhaust simulating introduction of added HC reductant. The gas flow rate was 1–2 L min^{-1}. The plasma was held at 180°C, a typical temperature for that of exhaust-treatment systems on a modern diesel-engine vehicle.

Figure 2 is a sketch of the dielectric barrier discharge device used to generate the plasma. It consists of two sheets of alumina, 24 × 100 × 1 mm. Each sheet has a platinum electrode embedded in the center. The two sheets are bonded together with a ceramic adhesive, leaving a gap of 1.3 mm between the sheets. The assembly is mounted in a quartz tube such that all the gas must flow through the gap between the sheets. The gas mixtures passed through the plasma with a space velocity of (25–50) × 10^3 h^{-1}. The two electrodes are connected to a Trek 10/10 high voltage amplifier driven by an HP33120A function generator. For these tests, the excitation wave was a triangle wave with peak voltage between 10 and 18 kV peak to peak at 32–500 Hz, adjusted such that energy deposition was 15–90 J L^{-1} of gas flow when the plasma was turned on.

Description of the Model

The plasma chemical processes were simulated using GLOBAL_KIN, a well stirred reactor model [14,15]. GLOBAL_KIN contains a self-consistent accounting of electron impact, ion–molecule, and neutral chemistry for the atmospheric pressure plasma chemistry of interest to this study. GLOBAL_KIN includes a solution of Boltzmann's equation for the electron energy distribution from which electron impact rate coefficients are obtained, a circuit module to provide electric fields within the plasma and address charging of surfaces in the dielectric barrier discharge, and a plasma chemistry module which addresses the gas phase reaction mechanism. GLOBAL_KIN was developed to investigate the plasma chemistry of gas mixtures such propane/propene/NO_x/N_2/O_2/H_2O, and in doing so extensive reaction mechanisms have also been developed, which are described in Refs [14–16]. GLOBAL_KIN is a zero-dimensional model which assumes homogeneous gas mixtures. While nonthermal atmospheric pressure plasma systems have a significant degree of heterogeneity, it has been shown that GLOBAL_KIN provides useful insight into the chemical and physical processes occurring in such systems [14–16]. The plasma chemistry model comprises 60 electron-impact reactions and nearly 390 heavy-species reactions, including ion–molecule processes. Kinetic data for reactions (1) and (2) were taken from Appendix, all other kinetic and mechanistic parameters were taken from the literature as described elsewhere [14–16].

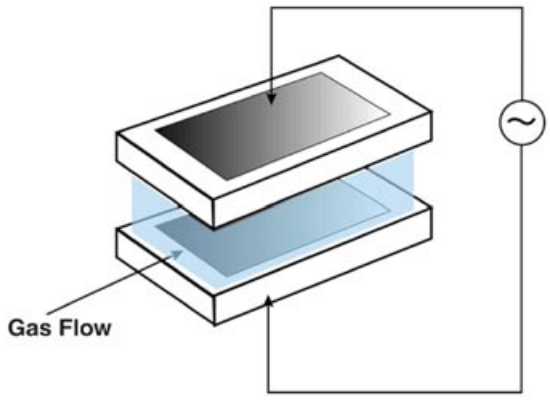

Figure 2 Sketch of the dielectric barrier discharge device.

Electron impact cross sections and ion–molecule rate coefficients for reactions directly with acetylene or propene are generally not available, and were not included in the model. In modeling similar systems addressing remediation of both volatile and nonvolatile hydrocarbons, extensive parameterizations were performed whereby electron-impact and ion–molecule reactions were included using a range of both measured and estimated rate coefficients as large as gas kinetic [17]. Based on these studies, we conclude that for these conditions, neutral driven chemistry is the far more likely reaction channel for the elimination of acetylene or propene. It is possible that there is a very rapid or resonant electron-impact process or ion–molecule reaction, which would preferentially deplete acetylene or propene; and if so our conclusions may need to be modified.

RESULTS

Results from the Experiments

To provide insight into the importance of O(^{3}P) atoms and OH radicals in the plasma, the relative consumption of propene (C_3H_6) and acetylene (C_2H_2) was monitored. The methodology used here is essentially the inverse of that used in a relative rate kinetic study. In a relative rate study the rate constant of interest is

measured relative to a reference reaction whose rate constant has already been established [18]. Experimental conditions are chosen such that the reactant and reference species are lost only via reaction with the radical of interest and that neither reactant, nor reference, are reformed in any process. Providing the reactant and reference have equal exposure to the radicals, it can be shown [18] that

$$\ln\left(\frac{[\text{reactant}]_{to}}{[\text{reactant}]_{t}}\right) = \frac{k_{react}}{k_{ref}}\ln\left(\frac{[\text{reference}]_{to}}{[\text{reference}]_{t}}\right)$$

where $[\text{reactant}]_{to}$, $[\text{reactant}]_{t}$, $[\text{reference}]_{to}$, and $[\text{reference}]_{t}$ are the concentrations of reactant and reference before and after exposure to the radical, and k_{react} and k_{ref} are the rate constants for reactions of the radical with the reactant and reference. Slopes of plots of the loss of reactant versus reference give the rate constant ratio k_{react}/k_{ref}. In the present work, the observed relative loss rates of acetylene and propene were compared to literature data for k_1/k_2 and k_3/k_4 to infer the relative importance of reaction with $O(^3P)$ atoms and OH radicals as losses of the organics.

$$O(^3P) + C_2H_2 \rightarrow \text{products} \quad (1)$$

$$O(^3P) + C_3H_6 \rightarrow \text{products} \quad (2)$$

$$OH + C_2H_2 \rightarrow \text{products} \quad (3)$$

$$OH + C_3H_6 \rightarrow \text{products} \quad (4)$$

Acetylene was chosen as "reactant" and propene was selected to be the "reference" for three reasons. First, these two compounds have different reactivities toward $O(^3P)$ atoms and OH radicals. Second, these two compounds can be monitored with high precision by FTIR spectroscopy. Third, they are readily available as high purity gas mixtures which can be handled conveniently by the experimental system. The literature data for k_1 [19–31] and k_2 [32–41] are discussed in the Appendix. For the present experimental conditions (453 K in 760 Torr of N_2 diluent) values of $k_1 = 9.2 \times 10^{-13}$, $k_2 = 4.6 \times 10^{-12}$, $k_3 = 1.45 \times 10^{-12}$ [42], and $k_4 = 1.47 \times 10^{-11}$ cm^3 molecule^{-1} s^{-1} [42] were used; we ascribe 20% uncertainty ranges for k_1–k_4. The relative reactivities of acetylene and propene towards $O(^3P)$ atoms and OH radicals are significantly different: $k_1/k_2 = 0.20 \pm 0.06$ and $k_3/k_4 = 0.099 \pm 0.028$.

Figure 3 shows the observed loss of acetylene versus that of propene resulting from passage of gas mixtures containing propene and acetylene through the plasma, using a variety of different experimental conditions. Data points near the origin are representative of experiments in which there were small losses of the organic compounds. Data points towards the top right-hand corner are those in which a large consumption of the organics was observed. The fractional consumption of propene is plotted along the x axis and that of acetylene is plotted along the y axis. This method of displaying the data renders an easy comparison of the relative losses of the organics in experiments using widely different initial concentrations of the organics.

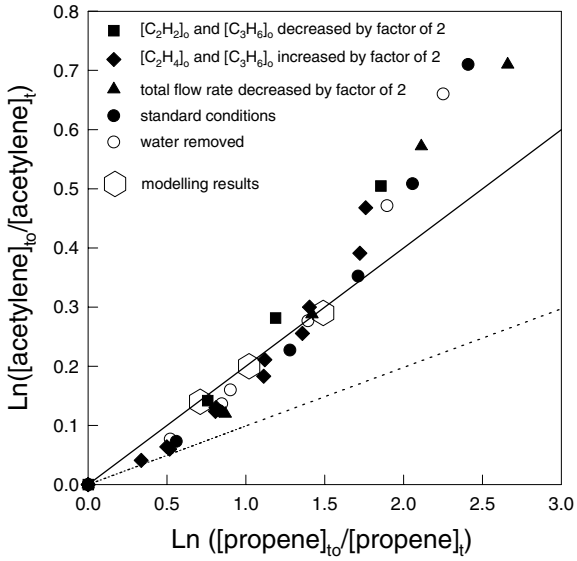

Figure 3 Loss of acetylene and propene following passage of gas mixtures through the nonthermal plasma at a total pressure of 1 atmosphere at 453 K (see text for details). The solid line shows the expected behavior if reaction with $O(^3P)$ atoms was the only loss of acetylene and propene. The dotted line shows the expected behavior if reaction with OH radicals was the only loss of acetylene and propene.

Filled circles in Fig. 3 show results obtained using "standard" conditions employing mixtures containing 260 ppm NO, 2% water vapor, 8% O_2, 1000 ppmC_1 acetylene, and 1000 ppmC_1 propene in one atmosphere total pressure of N_2 diluent at 180°C. The unit "ppmC_1" refers to a detector response equivalent to that given by the same concentration of a hydrocarbon containing one carbon atom (i.e. CH_4). The total flow rate was 2 L min^{-1}. The energy deposited into the gas by the plasma was 15–60 J L^{-1}. Open circles show the results obtained when water was removed from the reaction mixture (all other conditions remaining constant). The triangles show the behavior observed using energies of 30–60 J L^{-1} with the total flow decreased to 1 L min^{-1}. The diamonds and squares show the results obtained using "standard" conditions but with the initial concentration of acetylene and propene either increased (diamonds) or decreased (squares) by a factor of 2. The solid and dotted lines drawn through the origin in Fig. 3 have slopes of 0.20 and 0.099 and reflect

the expected behavior if acetylene and propene were consumed *exclusively* via reaction with either O(^{3}P) atoms or OH radicals, respectively. In addition to O(^{3}P) atoms and OH radicals, many other reactive species (such as O_2 ($^1\Delta_g$), NO_3, and O_3) may be formed in the plasma. These species have reactivities with C_2H_2 or C_3H_6, which are very different from those of O(^{3}P) atoms and OH radicals. For example, if reaction with O_3, NO_3, or O_2 ($^1\Delta_g$) was responsible for the loss of acetylene and propene, the data plot in Fig. 3 would have a slope of approximately 0.001, 0.04, or 8, respectively [41]. Inspection of Fig. 3 shows that this is clearly not the case and consequently that it is unlikely that the reactions with O_3, NO_3, or O_2 ($^1\Delta_g$) are important loss mechanisms for acetylene and propene. For propene consumptions of <85% (i.e., <2 on the x-axis scale in Fig. 3) the experimental data fall close to the solid line. This observation suggests, but does not prove, that under these experimental conditions the loss of both C_2H_2 and C_3H_6 are dominated by reaction with O(^{3}P). For propene consumptions of >85%, the experimental data lie significantly above the solid line suggesting that loss of C_2H_2 via processes other than reaction with O(^{3}P) are important.

Three additional conclusions can be drawn from the data in Fig. 3. First, the presence of water has no discernable impact on the relative consumption of the hydrocarbons. Addition of water was observed to increase the power required to reach a given level of hydrocarbon removal. This trend is a consequence of the large rate of electron dissociative attachment of and momentum transfer to water molecules. The loss of electrons to the formation of negative ions increases the impedance of the plasma. Although electron-impact dissociation of water does produce OH radicals, the rate of production of these radicals is not sufficient to significantly affect the net rate of removal of acetylene and propene. If reactions with OH radicals produced by electron-impact on water were important, the data acquired in the presence of water vapor would lie closer to the dotted line than the data acquired under dry conditions. Inspection of Fig. 3 shows that this is not the case and consequently that electron-impact dissociation of water is not a major factor in the plasma chemistry. Second, there is no discernable effect of variation of the initial hydrocarbon concentrations by a factor of 4. The gross features of the decays of acetylene and propene do not appear to be sensitive to the initial hydrocarbon concentration. Third, there is a discernable curvature to the plot. For the lowest consumptions of the organics the data lie between the solid and dotted lines, with increasing consumption the data tend toward the solid line. The simplest interpretation of this observation is that O(^{3}P) atoms and OH radicals play important roles in the initiation of acetylene and propene in the system and the relative importance of O(^{3}P) atoms increases with the degree of consumption of the organics. The curvature of the data plot in Fig. 3 evident at low HC conversions can be explained qualitatively by considering the fundamentally different nature of the sources of O(^{3}P) atoms and OH radicals in the system. O(^{3}P) atoms are formed via dissociation of O_2 caused by electron-impact. There are no known chemical reactions that form O(^{3}P) atoms in the system. In principal there is a direct mechanism by which the electrical discharge can form OH radicals in the system via H_2O dissociation.

$$e + H_2O \rightarrow H + OH + e \qquad (5)$$

However, as discussed earlier, the experimental evidence suggests that such direct formation of OH is not important. There are two principal indirect sources of OH radicals: abstraction of H atoms from organic species by O atoms (for example in reaction with CH_3CHO) and reaction of HO_2 radicals with NO.

$$O + CH_3C(O)H \rightarrow CH_3C(O) + OH \qquad (6)$$

$$HO_2 + NO \rightarrow OH + NO_2 \qquad (7)$$

It is interesting to contrast the fact that O atoms are formed directly by the plasma, whereas OH radicals are formed indirectly as a result of reactions initiated by the O atom attack on the hydrocarbons.

As the plasma power or gas residence time increases, the conversion of hydrocarbon increases, the concentration of NO decreases, the importance of the $HO_2 + NO$ reaction decreases, and hence the importance of OH radicals will decrease—consistent with the data trend in Fig. 3. Furthermore, as mentioned in the Introduction section, the chemistry occurring in the plasma converts NO into NO_2. As the concentration of NO_2 increases, loss of OH radicals via reaction (8) may become increasingly important and the relative contribution of OH radicals to the loss of hydrocarbons may decrease.

$$OH + NO_2 + M \rightarrow HNO_3 + M \qquad (8)$$

As noted earlier, for propene conversions of >85%, the data lie significantly above the solid line indicating that at least one other species in addition to O(^{3}P) is responsible for the loss of organics. The identity of this additional loss mechanism is unknown.

Results from the Global Modeling

To help interpret the experimental results, global modeling of the reaction chemistry was performed using GLOBAL_KIN. With the initial concentrations of the

Table II Computed Fractional Loss of C_2H_2 and C_3H_6

Energy Deposition (J L^{-1})	% C_2H_2 Loss Attributable to Reaction With			% C_3H_6 Loss Attributable to Reaction With		
	$O(^3P)$	OH	$O(^3P)$ + OH	$O(^3P)$	OH	$O(^3P)$ + OH
47	72	28	100	55	45	100
70	74	26	100	62	38	100
93	76	24	100	66	34	100

reactants as in Table I, three model runs were conducted with total energy depositions of 47, 70, and 93 J L^{-1}. Chemical reactions of acetylene in the model included loss via reactions with $O(^3P)$, OH, HO_2, and CH_3. Chemical reactions of propene in the model included loss via reactions with $O(^3P)$, OH, and H.

It was found that of the loss mechanisms considered, the reactions with $O(^3P)$ and OH were responsible for essentially all (>99.99%) of the loss of both acetylene and propene. Plasma deposition energies of 47, 70, and 93 J L^{-1} resulted in consumptions of 13%, 18%, and 25% of the initial acetylene, and 49%, 64%, and 77% of the initial propene. These results are plotted as open hexagons in Fig. 3. The relative contributions from $O(^3P)$ atoms and OH radicals towards the oxidation of acetylene and propene are listed in Table II. The results from the computational investigation are consistent with those from the experimental study, namely, that $O(^3P)$ atoms and, to a lesser extent, OH radicals are the major species responsible for initiating the oxidation of acetylene and propene in the plasma.

DISCUSSION

The results of an experimental and computational study provide a consistent picture of the importance of $O(^3P)$ atoms and OH radicals as initiation agents in the oxidation of acetylene and propene in simulated diesel exhaust. The data suggest that both $O(^3P)$ atoms and, to a lesser extent, OH radicals contribute to hydrocarbon oxidation with the relative importance of $O(^3P)$ atoms increasing with the degree of plasma processing of the gas mixtures (i.e., with plasma power and residence time of gas in the plasma). It is interesting to compare this finding with the situation in combustion chemistry where OH radicals, H atoms, and, to a lesser extent, $O(^3P)$ atoms initiate the hydrocarbon oxidation. It appears that the relative importance of $O(^3P)$ atoms and OH radicals is different in the two cases. In view of the different physical and chemical environments and radical sources, it is perhaps not surprising that there are significant differences in the relative importance of $O(^3P)$ atoms and OH radicals in combustion and plasma systems.

The average $O(^3P)$ atom concentration in the plasma used in the present work can be estimated from the observed propene consumption. For the standard mixture (including water vapor) with 60 J L^{-1} specific energy deposition, the propene consumption was typically approximately 75% (corresponding to an x-axis value of approximately 1.4 in Fig. 3). The residence time in the plasma was 0.072 s (space velocity = 50,000 h^{-1}). Attributing all of the propene loss to reaction with $O(^3P)$ atoms, assuming a homogeneous steady state $O(^3P)$ atom concentration, and adopting $k_2 = (4.6 \pm 0.9) \times 10^{-12}$ cm^3 $molecule^{-1}$ s^{-1} leads to an estimate of $[O(^3P)]$ of approximately 4×10^{12} cm^{-3}.

The present work provides a framework for understanding the chemical processes responsible for hydrocarbon oxidation in nonthermal plasma systems. To the best of our knowledge, the present work is the first experimental demonstration of the importance of $O(^3P)$ atoms and OH radicals in the initiation of hydrocarbon oxidation during nonthermal plasma treatment of diesel exhaust.

Finally, the present work illustrates a novel application of the relative-rate technique. The methodology used here is essentially the inverse of that used in a relative rate kinetic study. In typical relative rate studies, the reactive species are known and the relative losses of reference and reactant compounds are used to provide kinetic information. In the present work the kinetics of the reactions are taken from the literature and the relative losses of reference and reactant compounds are used to provide information concerning the identity of the reacting species.

APPENDIX: REVIEW OF LITERATURE DATA FOR $k(O(^3P) + C_2H_2)$ AND $k(O(^3P) + C_3H_6)$

Absolute rate literature data reported for k_1 and k_2 are plotted in Figs. A1 and A2.

$$O(^3P) + C_2H_2 \rightarrow \text{products}$$

$$O(^3P) + C_3H_6 \rightarrow \text{products}$$

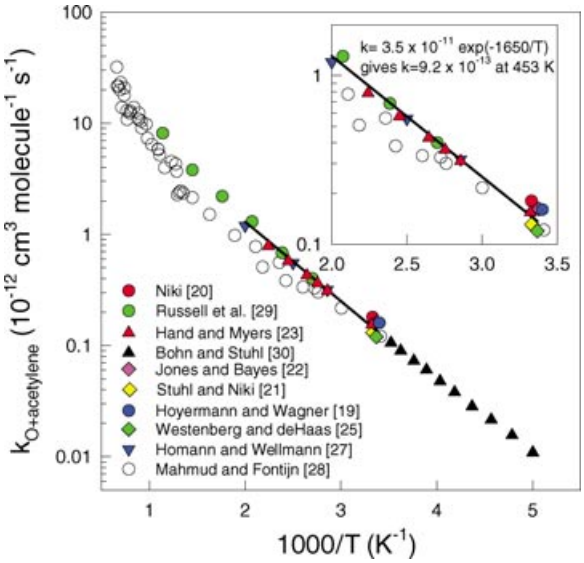

Figure A1 Kinetic data for reaction of O(^{3}P) atoms with acetylene. The line is a linear least-squares fit (see text for details).

The inserts in Figs. A1 and A2 show the data measured over the temperature range of 295–500 K, which is of most relevance to the present discussions. As can seen from Fig. A1, with the exception of the work of Mahmud and Fontijn [28] (open circles) there is an excellent agreement in the literature data for k_1. In the present work we are interested in the value of k_1 at 453 K. Linear least-squares analysis of the available data in the temperature range of 295–500 K (Mahmud and Fontijn [28] data excepted) gives $k_1 = 3.5 \times 10^{-11}$ exp($-1650/T$) and is plotted as the solid line in Fig. A1, which gives $k_1 = 9.2 \times 10^{-13}$ cm^3 molecule^{-1} s^{-1} at 453 K.

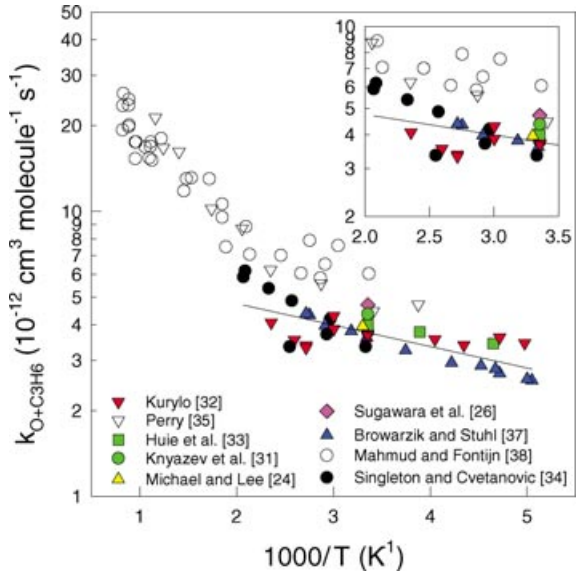

Figure A2 Kinetic data for reaction of O(^{3}P) atoms with propene. The line is a linear least-squares fit (see text for details).

Figure A2 shows the available data for k_2. The results of Mahmud and Fontijn [38] (open circles) and Perry [35] (open triangles) are significantly higher values than those in other studies. In addition to the absolute rate data in Fig. A2, relative rate techniques have established that $k_2/k_9 = 0.23$ at room temperature [39].

$$\text{O}(^3\text{P}) + \text{2-methylpropene} \rightarrow \text{products} \qquad \text{(A1)}$$

Using $k_9 = 1.69 \times 10^{-11}$ [40] gives $k_2 = 3.9 \times 10^{-12}$ cm^3 molecule^{-1} s^{-1}, which is consistent with all studies except that of Mahmud and Fontijn [38]. Linear least-squares analysis of the available data in the temperature range of 200–500 K (Mahmud and Fontijn [38] and Perry [35] data excepted) gives $k_2 = 6.7 \times 10^{-12}$ exp($-170/T$) and is plotted as the solid line in Fig. A2. At 453 K this gives $k_2 = 4.6 \times 10^{-12}$ cm^3 molecule^{-1} s^{-1}.

BIBLIOGRAPHY

1. Penetrante, B. M.; Brusasco, R. M.; Pitz, W. J.; Vogtlin, G. E.; Kung, M. C.; Kung, M. H.; Wan, C. Z.; Voss, K. E. Paper number 982508; Society of Automotive Engineers, October 1998.
2. Hoard, J. W.; Balmer, M. L. Paper number 982429; Society of Automotive Engineers, October 1998.
3. Balmer, M. L.; Tonkyn, R.; Kim, A.; Yoon, S.; Jiminez, D.; Orlando, T. M.; Barlow, S. E. Paper number 982511; Society of Automotive Engineers, October 1998.
4. Shimizu, S.; Oda, T. Denki Gakkai Hoden Kenkyukai Shiryo 1997, ED-97(209–225), 39–44 (in Japanese).
5. Fisher, G. B.; DiMaggio, C. L.; Yezerets, A.; Kung, M. C.; Kung, H. H.; Baskaran, S.; Frye, J. G.; Smith, M. R.; Herling, D. R.; LeBarge, W. J.; Kupe, J. Paper number 2000-01-2965; Society of Automotive Engineers, 2000.
6. Schmieg, S.; Cho, B.; Oh, S. Paper number 2001-01-3565; Society of Automotive Engineers, 2001.
7. Hoard, J. W.; Panov, A. Paper number 2001-01-3512; Society of Automotive Engineers, 2001.
8. Panov, A.; Tonkyn, R. G.; Balmer, M. L.; Peden, C. H. F.; Malkin, A.; Hoard, J. W. Paper number 2001-01-3513; Society of Automotive Engineers, 2001.
9. Kogelschatz, G.; Eliasson, B.; Hirth, M. J Phys D: Appl Phys 1987, 20, 1421.
10. Herron, J. T.; Huie, R. E. J Phys Chem Ref Data 1974, 2, 467.
11. Brasseur, G. P.; Orlando, J. J.; Tyndall, G. S. Atmospheric Chemistry and Global Change; Oxford University Press: Oxford, UK, 1999.

12. Hoard, J. W.; Wallington, T. J.; Ball, J. C.; Hurley, M. D.; Wodzisz, K.; Balmer, M. L. Environ Sci Technol 1999, 33, 3427.
13. Gierczak, C. A.; Andino, J. M.; Butler, J. W.; Heiser, G. A.; Jession, J.; Korniski, T. J. Measurement of Atmospheric Gasses; The International Society for Optical Engineering, 1991; Vol. 1433, 315 p.
14. Dorai, R.; Kushner, M. J. J Appl Phys 2000, 88, 3739.
15. Dorai, R.; Kushner, M. J. J Phys D 2001, 34, 574.
16. Dorai, R. Modeling of Atmospheric Pressure Plasma Processing of Gases and Surfaces, PhD Thesis; University of Illinois, Urbana, 2002; ftp://uigelz.ece.uiuc.edu/pub/theses.html.
17. Williams, S.; Arnold, S.; Viggiano, A. A.; Morris, R.; Dorai, R.; Kushner, M. J. In 52nd Gaseous Electronics Conference, Norfolk, VA, October 1999; Bull Am Phys Soc 1999, 44, 57.
18. Atkinson, R. Chem Rev 1986, 86, 69.
19. Hoyermann, K.; Wagner, H. Gg. Z Phys Chem 1967, 55, 72.
20. Niki, H. J Chem Phys 1967, 47, 3102.
21. Stuhl, F.; Niki, H. J Chem Phys 1971, 55, 3954.
22. Jones, I. T. N.; Bayes, K. D. Proc R Soc London A 1973, 335, 547.
23. Hand, C. W.; Myers, R. M. J Phys Chem 1976, 80, 557.
24. Michael, J. V.; Lee, J. H. Chem Phys Lett 1977, 51, 303.
25. Westenberg, A. A.; deHaas, N. J Chem Phys 1977, 66, 4900.
26. Sugawara, K.; Ishikawa, Y.; Sato, S. Bull Chem Soc Jpn 1980, 53, 1344.
27. Homann, K. J.; Wellmann, Ch. Ber Bunsenges Phys Chem 1983, 87, 527.
28. Mahmud, M.; Fontijn, A. J Phys Chem 1987, 91, 1918.
29. Russell, J. J.; Senkan, S. M.; Seetula, J. A.; Gutman, D. In Proceedings of 22nd Symposium on Combustion, 1988; p. 1007.
30. Bohn, B.; Stuhl, F. J Phys Chem 1990, 94, 8010.
31. Knyazev, V. D.; Arutyunov, V. S.; Dedeneev, V. I. Int J Chem Kinet 1992, 24, 545.
32. Kurylo, M. J. Chem Phys Lett 1972, 14, 117.
33. Huie, R. E.; Herron, J. T.; Davis, D. D. J Phys Chem 1972, 76, 3311.
34. Singleton, D. L.; Cvetanovic, R. J. J Am Chem Soc 1976, 98, 6812.
35. Perry, R. A. J Chem Phys 1984, 80, 153.
36. Atkinson, R.; Pitts, J. N. Jr. J Chem Phys 1977, 67, 38.
37. Browarzik, P.; Stuhl, F. J Phys Chem 1984, 88, 6004.
38. Mahmud, K.; Fontijn, A. In Proceedings of 22nd Symposium on Combustion, 1988; p. 991.
39. Cvetanovic, R. J. Can J Chem 1960, 38, 1678.
40. Atkinson, R. J Phys Chem Ref Data 1997, 26, 215.
41. Westley, F.; Herron, J.; Frizzell, D. NIST Standard Kinetics Database 17-2Q98; Gaithersburg, MD, 1998.
42. Atkinson, R. J Phys Chem Ref Data 1989, Monograph 1.